DOI: 10.1002/anie.200703244

Thienyl Biradicals

On the Biradicaloid Nature of Long Quinoidal Oligothiophenes: Experimental Evidence Guided by Theoretical Studies**

Rocío Ponce Ortiz, Juan Casado, Víctor Hernández, Juan T. López Navarrete, Pedro M. Viruela, Enrique Ortí,* Kazuo Takimiya, and Tetsuo Otsubo*

Quinoidal oligothiophenes were recently found to be promising semiconductor components in organic field effect transistors (OFETs) for molecular electronics.[1] Initially, they emerged as excellent n-channel actuators but soon surpassed the most optimistic predictions when ambipolar (n and p) behavior was achieved.[2] Today, they might exemplify the concept of functional materials, owing to the new and challenging finding that they also display magnetic activity, a quite unusual property for pure, neutral organic compounds.[3] A main drawback, however, is their complicated synthesis, which explains the fact that the first examples were not longer than tetramers (a 96-mer has been obtained for the aromatic analogues).[4] Recently, a full series of quinoidal oligothiophenes Q*n* ($n = 1$–6, Scheme 1) end-capped with dicyanomethylene groups have been prepared and were reported to display tunable ESR activity as a function of the number of thienoquinoid units.[5] While Q1–Q4 are ESR-silent, Q5 and Q6 present a broad ESR signal at $g = 2.0033$ and are suggested to be in equilibrium with a biradical species in 2.8% and 29% proportions, respectively. The existence of a second species is supported by the evolution of the electronic spectra with temperature.[5] This uncommon behavior is also found for their structural properties, since, as described below, their Fourier transform Raman spectra change with oligomer size, a behavior never observed for aromatic oligothiophenes. Moreover, the dependence of the Raman bands on temperature and the drastic change they exhibit when the wavelength of laser excitation is changed is also unusual. The objective of this work is twofold. First, we investigate a molecular mechanism able to account simultaneously for the magnetic and spectral findings. Second, we illustrate the versatility of Raman spectroscopy to extract fruitful information on enigmatic molecular properties related to the electronic structure of π-conjugated systems with extremely small band gaps.

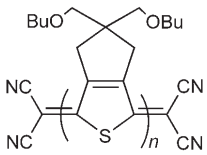

Q*n* (*n* = 1-6)

Scheme 1. Chemical structures of Q1–Q6.

The electronic structure of compounds Q1 to Q6 was first investigated at the restricted RB3LYP/6-31G** level of theory (computational details are given in the Supporting Information). The energy gaps between the highest occupied and lowest unoccupied molecular orbitals (HOMO and LUMO) that we find for the Q*n* members are very small (Q1: 2.90 eV, Q2: 2.16 eV, Q3: 1.67 eV, Q4: 1.33 eV, Q5: 1.06 eV, Q6: 0.83 eV); indeed, they are much smaller than those computed for aromatic oligothiophenes (T*n*; e.g. 3.45 eV for T3 and 3.09 eV for T4, see Figure S1 in the Supporting Information). The HOMO–LUMO gaps predicted for Q*n* agree with the small electrochemical gaps inferred from redox potentials (Q3: 1.46 eV, Q4: 1.01 eV, Q5: 0.71 eV, Q6: 0.50 eV) and the low-energy absorption maxima observed in the electronic spectra (Q3: 1.89 eV, Q4: 1.57 eV, Q5: 1.36 eV, Q6: 1.23 eV).[5]

In general, the electronic ground state of compounds with large HOMO–LUMO gaps is well described by a single, closed-shell electron configuration $^1\Phi_0$. In contrast, electrons in compounds with small HOMO–LUMO gaps are easily promoted from the HOMO to the LUMO, and the ground state of the system may present increasing biradical character as the HOMO–LUMO gap decreases. Such biradical character has been recently demonstrated for phenalenyl-based polycyclic hydrocarbons containing a *p*-quinodimethane central unit.[6] The singlet ground state S_0 of compounds Q1–Q6 is therefore proposed to be represented by the resonance of the closed-shell quinoid Kekulé structure and the biradical form given in Scheme 2. The relative weight of these two forms would determine the biradical contribution to the electronic ground state. However, this situation is magnetically silent, and the existence of a magnetically active triplet state (T_1) is mandatory to account for the experimental ESR activity. Hence, the S_0 state is proposed to be in thermal equilibrium with a T_1 state that is energetically populated at room temperature.

[*] R. Ponce Ortiz, Dr. J. Casado, Prof. V. Hernández, Prof. J. T. López Navarrete
Department of Physical Chemistry
University of Málaga
Campus de Teatinos s/n, 29071-Málaga (Spain)
Fax: (+34) 952132000
E-mail: teodomiro@uma.es
Prof. P. M. Viruela, Prof. E. Ortí
Instituto de Ciencia Molecular
Universidad de Valencia
P.P Box 22085, 46071-Valencia (Spain)
Fax: (+34) 963543274
E-mail: enrique.orti@uv.es
Dr. K. Takimiya, Prof. T. Otsubo
Department of Applied Chemistry
Hiroshima University
Higashi-Hiroshima 739-8527 (Japan).

[**] This work was supported by the Ministerio de Educación y Ciencia (MEC) of Spain and by FEDER funds (project CTQ2006-14987). J.C. is indebted to the MEC for an I3 position of Chemistry at the University of Málaga. R.P.O. thanks the Junta de Andalucía for a personal doctoral grant.

Supporting information for this article is available on the WWW under http://www.angewandte.org or from the author.

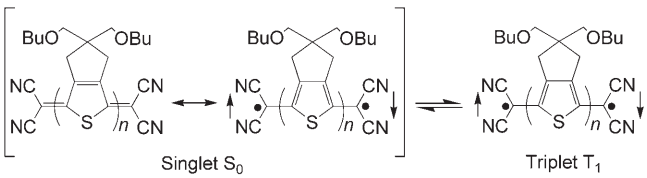

Scheme 2. Kekulé and biradical resonance structures proposed for the singlet ground state of compounds Q1–Q6 in equilibrium with the triplet species.

The biradical character of S_0 was investigated by reoptimizing the geometry of compounds Q1–Q6 using an unrestricted (U) broken-symmetry (BS) wave function (UB3LYP(BS)/6-31G**). For the shorter oligomers Q1–Q3, the UB3LYP(BS) solution converges to the RB3LYP geometry, and a closed-shell quinoidal Kekulé structure is predicted as the ground state (see Figure S2 in the Supporting Information). For the longer oligomers Q4–Q6, the restricted wave function shows a restricted→unrestricted instability, and the open-shell UB3LYP(BS) solution becomes lower in energy than the closed-shell RB3LYP one by 0.41 (Q4), 2.03 (Q5), and 4.10 kcal mol^{-1} (Q6, Table 1). This result means that the biradical form contributes to the ground-state structure of Q4–Q6, and that the contribution increases with the number of thienyl units.[7]

Table 1: Relative energies (in kcal mol^{-1}) for the S_0 and T_1 states for compounds Q1 to Q6. Spin contamination ($\langle S^2 \rangle$) is given for S_0.[a]

Compound	ΔE(CS−OS)[b]	$\langle S^2 \rangle$	$\Delta E(T_1-S_0)$[c]
Q1	0.00	0.00	27.24
Q2	0.00	0.00	16.97
Q3	0.00	0.00	9.88
Q4	0.41	0.51	5.07
Q5	2.03	0.86	2.60
Q6	4.10	1.00	1.35

[a] Calculated at the B3LYP/6-31G** level. [b] Closed-shell (CS) RB3LYP singlet energy minus open-shell (OS) UB3LYP(BS) singlet energy. [c] UB3LYP triplet energy minus singlet energy (OS singlet for Q4, Q5, and Q6).

The degree of singlet biradical character was estimated by performing CASSCF(2,2)/6-31G single-point calculations at the UB3LYP(BS)/6-31G** optimized geometries. CASSCF calculations provide an admixture of the doubly-excited configuration $^1\phi_{H,H\rightarrow L,L}$ into the singlet ground state. This admixture amounts to 4% for Q4, 34% for Q5, and 45% for Q6, which correspond to LUMO occupation numbers of 0.08, 0.68, and 0.90 e, respectively. Thus, the singlet biradical character of S_0 is estimated to be 8% for Q4, 68% for Q5, and 90% for Q6.[8]

Calculations therefore predict that the transition towards the open-shell singlet ground state starts at Q4, which shows a low degree of biradical character. The UB3LYP(BS) geometry of Q4 is indeed similar to that obtained at the RB3LYP level, and the structure remains highly quinoidal (see Figure S3 in the Supporting Information). The quinoidal character is reduced for Q5 and Q6, which present partially aromatized geometries owing to the large contribution of the biradical form (see Figure S4 and Table S2 in the Supporting Information).

Investigation of the frontier molecular orbitals gives additional insight into the nature of the open-shell ground state. Figure 1 displays the two singly occupied molecular orbitals (SOMOs) calculated for Q6 at the UB3LYP(BS)/6-31G** level. They are essentially confined on the two halves of the molecule with almost no overlap between them. The unpaired electrons therefore reside on different parts of the molecule, and Q6 can be classified as a singlet disjoint biradical.[9]

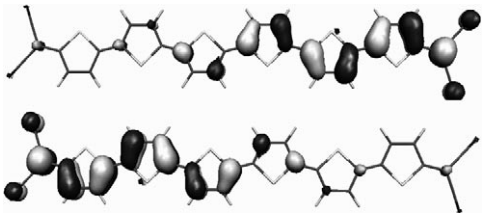

Figure 1. Electron-density contours (0.03 e bohr^{-3}) calculated at the UB3LYP(BS)/6-31G** level for the singly occupied molecular orbitals of Q6. Bis(butoxymethyl)cyclopentane moieties are omitted, because they show no contribution.

The triplet T_1 state is always calculated to be higher in energy than the singlet S_0 state (see Table 1). The energy difference decreases rapidly with increasing oligomer length, and the T_1 state is only slightly higher in energy than the open-shell S_0 state for Q5 (2.60 kcal mol^{-1}) and Q6 (1.35 kcal mol^{-1}). These findings indicate that the ground state of quinoidal oligothiophenes Q*n* is always a singlet, and that this singlet state is in thermal equilibrium with a low-energy triplet state for the longest oligomers at room temperature.[10] The populations estimated for the T_1 state using a Boltzmann distribution and the calculated energy differences $\Delta E(T_1-S_0)$ are 3.6% for Q5 and 24% for Q6. These populations are in good agreement with the experimental values inferred from ESR intensities (2.8 and 29%, respectively) and explain the magnetic activity observed for Q5 and Q6.[5] For Q4, the calculated $\Delta E(T_1-S_0) = 5.07$ kcal mol^{-1} leads to a T_1 population of only 0.06%, and no ESR signal is detected. As shown in Figure S5 in the Supporting Information for Q6, the atomic spin densities calculated for the T_1 state increase in going from the center to the ends of the molecule, and the unpaired electrons are mainly concentrated on the outer thiophene rings (0.30 spins per ring) and on the terminal $C(CN)_2$ groups (0.49 spins per group). Thus, the triplet T_1 state is best described as the biradical sketched in Scheme 2.

The molecular structures of compounds Q*n* become more aromatic in the T_1 state (see Figures S2–S4 in the Supporting Information). The degree of aromatization decreases in going from the inner to the outer thiophene rings. For Q6, the geometry of the T_1 state resembles the open-shell geometry of the S_0 state (maximum bond-length differences of 0.010 Å) owing to the high biradical character of the S_0 state. This geometric feature will indeed be the connection that allows us to understand the Raman spectra discussed below, which will

clarify the balanced quinoid and aromatic portions describing the S_0 geometry and the more aromatic character of T_1.

The electronic absorption spectra of Q*n* present an intense, structured band in the visible range that shifts to the near-infrared for the longest oligomers (Table 2).[5] Time-dependent RB3LYP calculations correctly predict the existence of this band, which is associated with the HOMO–LUMO excitation, and reproduce the transition energies quite well (Table 2). However, they do not account for the group of less intense bands that Q5 and Q6 present in the visible region (500–800 nm).[5] The excited states of Q5 and Q6 were thus recalculated at the UB3LYP(BS)/6-31G** level that takes into account the biradical character of S_0. Similarly to RB3LYP calculations, UB3LYP(BS) calculations predict an intense electronic transition in the near-infrared for Q5 (1.32 eV, 942 nm, $f = 1.46$) and Q6 (1.17 eV, 1057 nm, $f = 1.39$). In addition, they reveal new transitions in the visible region at 2.04 eV (607 nm) for Q5 and at 1.93 eV (641 nm) and 2.28 eV (543 nm) for Q6. These results agree with the experimental data and support the biradical character of S_0 predicted for Q5 and Q6 (see Figure S6 in the Supporting Information). For these oligomers, especially for Q6, the T_1 state is partially populated at room temperature and would also contribute to the electronic spectrum. Time-dependent UB3LYP/6-31G** calculations of the $T_1 \rightarrow T_n$ transitions for Q6 predict an intense $T_1 \rightarrow T_4$ transition at 1.72 eV (720 nm, $f = 2.03$) and two less-intense transitions at 1.13 (1095 nm, $f = 0.39$) and 2.35 eV (527 nm, $f = 0.56$). These results suggest that the molecules populating the T_1 state contribute both to the bands in the visible and to those in the near-infrared region.

Because the partial population of T_1 is in equilibrium with S_0, and because of the intense electronic transitions ($S_0 \rightarrow S_n$ and $T_1 \rightarrow T_n$) predicted and recorded for both species, it can be hypothesized that the Raman intensity will depend on the laser excitation wavelength. This intensity would vary depending on which species resonates for a given wavelength (i.e. resonant Raman conditions with the absorbing S_0 or T_1 states). If this effect really occurs, it should be most noticeable for Q6, for which the populations of both states are similar ($\Delta E(T_1 - S_0) = 1.35$ kcal mol^{-1}).

Figure 2 displays the Raman spectra for Q6 with laser energies chosen according to the T_1 or S_0 absorptions in the UV/Vis/NIR spectrum (see Figure S6 in the Supporting Information). The spectrum recorded with an excitation wavelength $\lambda_{exc} = 514$ nm (corresponding to the absorption predicted at 527 nm for T_1) is similar to that of aromatic oligothiophenes (the spectrum of α,α′-dimethylterthiophene (DMT3) is shown for comparison),[11] thus suggesting that the molecular structure of the T_1 state is of heteroaromatic nature, equivalent to that of an aromatic terthiophene. The spectrum recorded with $\lambda_{exc} = 1064$ nm (resonating with the $S_0 \rightarrow S_1$ absorption calculated at 1057 nm) is particularly similar to the spectrum of the radical cation of DMT6 (α,α′-dimethylhexathiophene), which displays quinoidal-type geometry in the central three or four rings and partially aromatic character for the outermost rings. This situation is equivalent to the picture provided theoretically for the S_0 species, whose geometry is not completely quinoidal but mixed with an aromatic portion owing the proaromatic open-shell singlet biradical. This analysis opens the question as to whether the "aromatic" bands at 1500–1450 cm^{-1} emerge from the aromatization process in the open-shell singlet biradical (S_0) or are due to the aromatic T_1 species (present in low proportion). This question is discussed below, but let us look first for spectroscopic verification of the coexistence of singlet and triplet species, which are proposed to be in thermal equilibrium.

Figure 3 shows the Raman spectra as a function of temperature for the two representative cases Q4 and Q6. According to calculations, the T_1 state of Q4 resides 5.07 kcal mol^{-1} above the S_0 state. Consequently, an increased population of T_1 at the expense of S_0 can be expected with increasing temperature. In the spectra, we should then observe a relative enhancement of "aromatic-triplet" bands at higher temperatures relative to the "quinoidal" bands,

Table 2: Observed and calculated transition energies (λ in nm, ΔE in eV) and oscillator strengths (f) for the most intense electronic absorption bands.

Compound	Exptl[a]		RB3LYP/6-31G**[b]		
	λ_{max}	ΔE	λ	ΔE	f
Q1	412	3.01	392	3.16	0.69
Q2	548	2.26	507	2.45	1.24
Q3	657	1.89	621	2.00	1.79
Q4	788	1.57	739	1.68	2.35
Q5	913	1.36	863	1.44 (1.32)	2.89 (1.46)
Q6	1012	1.22	1001	1.24 (1.17)	3.34 (1.39)

[a] Experimental data from reference [5] measured in THF. [b] Time-dependent RB3LYP/6-31G** calculations at the RB3LYP/6-31G** optimized energies. The data quoted are for the $S_0 \rightarrow S_1$ electronic transition ($S_0 \rightarrow S_3$ for Q1) that corresponds to the HOMO–LUMO excitation. Data from time-dependent UB3LYP(BS)/6-31G** calculations are given in parentheses for Q5 and Q6.

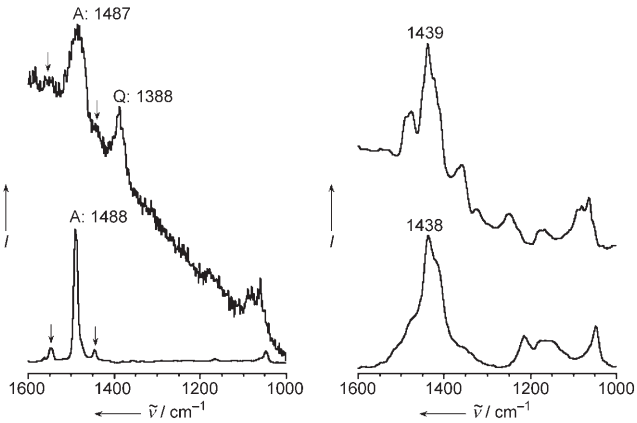

Figure 2. Raman spectra of Q6 with excitation at 514 nm (top left), DMT3 (exc 1064 nm, bottom left), Q6 with excitation at 1064 nm (top right), and radical cation of DMT6 (exc 1064 nm, bottom right). Q and A denote typical quinoidal and aromatic bands, respectively. The arrows highlight correlated weak bands.

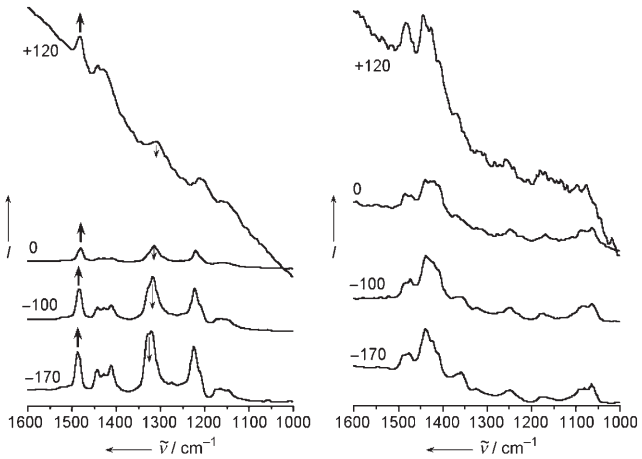

Figure 3. Raman spectra as a function of temperature (in °C) for Q4 (left) and Q6 (right). Arrows show band trends on heating.

which are predominant at lower temperatures. This behavior is reflected in Figure 3; the strongest quinoidal band around 1300 cm^{-1} (S_0 state) decreases in intensity relative to the aromatic feature at around 1490 cm^{-1} (which is mainly due to the T_1 species).

Since the T_1 state is much closer in energy to the singlet ground state in Q6 (1.35 kcal mol^{-1}) than in Q4, a rather different behavior would be anticipated for Q6 (no or minimal relative intensity dependence of the aromatic and quinoid bands on temperature). Indeed, the quinoid band at around 1400 cm^{-1} remains the strongest in the spectrum of Q6 for all temperatures.

It is challenging to find experimental Raman evidence supporting the contribution of the open-shell singlet biradical to the electronic structure of S_0, which was suggested by theoretical calculations and is shown in Scheme 2. DFT geometries predict an increasing degree of aromatization of the molecular structure upon increased participation of the aromatic-like biradical resonant form. For pure aromatic oligothiophenes (Figure 4, left), the strongest Raman bands (ring $\tilde{\nu}_s$(C=C)) are located in the interval 1500–1450 cm^{-1} and evolve to lower frequencies with increasing chain length. For Q3, DFT calculations exclude the participation of the aromatic biradical resonant structure, and its Raman spectrum (Figure 4, right) nominally corresponds to a fully quinoidal structure characterized by the most active Raman band under 1400 cm^{-1} (inter-ring $\tilde{\nu}_s$(C=C)). As a consequence, it can be argued that the appearance of active Raman bands in the aromatic $\tilde{\nu}_s$(C=C) frequency region in the longest Q*n* members indicates the aromatization of the S_0 state, arising from the contribution of the singlet biradical form. Raman spectra with excitation at 1064 nm (recorded at −150 °C to minimize the influence of triplet species) are shown in Figure 4; prominent Raman bands at 1488, 1462, and 1440–1420 cm^{-1} are observed for Q4, Q5, and Q6. With the assumption that these spectra belong to the S_0 species, the detection of aromatic bands in the spectra suggests the contribution of an aromatic biradical resonant form. The continuous downshift of these aromatic bands on moving from Q4 to Q6 (and thus extending electron delocalization), accompanied by an intensity enhancement, is likely an indication of the increasing weight of the singlet biradical form in longer oligomers, which is in agreement with DFT predictions. The same effect (restricted quinoidization at the expense of increased aromatization) pushes the quinoidal band from 1313 cm^{-1} in Q4 to 1381 cm^{-1} in Q5 and 1424 cm^{-1} in Q6. This result seems to indicate that in Q6, the contributions of quinodal and aromatic forms to S_0 are almost balanced; their associated signals nearly coalesce into one relevant Raman band halfway between the typical frequencies of pure aromatic and quinoidal bands.

In conclusion, we have presented a set of spectroscopic and theoretical evidence that supports the existence of very low energy, thermally accessible, excited triplet states, which are responsible for the magnetic activity in long quinoidal thienyl molecules. The results consistently describe the molecular and electronic structures of these compounds and the dramatic evolution they undergo with increasing oligomer length. Particularly interesting is the fact that the ground state has been shown to be always a singlet state, and that it presents biradicaloid character that increases with the chain length. The study shows that Raman spectroscopy is an extremely powerful and versatile tool to disentangle the electronic structure of biradicals, especially in the case of π-electron systems with very small band gaps.

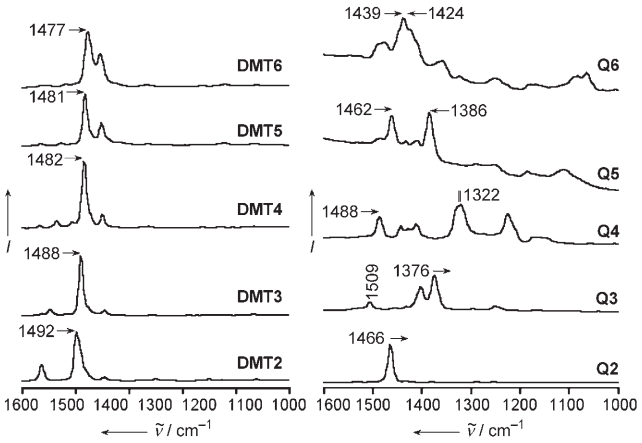

Figure 4. FT-Raman spectra with excitation at 1064 nm of aromatic dimethyl oligothiophenes (left, from a dimer to a hexamer) and of Q*n* (right, spectra recorded at −150 °C). Arrows indicate wavenumber trends on increasing chain length.

Received: July 19, 2007
Published online: October 25, 2007

Keywords: biradicals · density functional calculations · oligothiophenes · Raman spectroscopy · triplet excited states

[1] a) J. Casado, L. L. Miller, K. R. Mann, T. M. Pappenfus, H. Higuchi, E. Ortí, B. Millián, R. Pou-Amérigo, V. Hernández, J. T. López Navarrete, *J. Am. Chem. Soc.* **2002**, *124*, 12380–12388; b) T. M. Pappenfus, R. J. Chesterfield, C. D. Frisbie, K. R. Mann, J. Casado, J. D. Raff, L. L. Miller, *J. Am. Chem. Soc.* **2002**, *124*, 4184–4185; c) D. E. Jansen, . M. W. Burand, P. C. Ewbank, T. M.

Pappenfus, H. Higuchi, D. da Silva Filho, V. G. Young, J.-L. Brédas, K. R. Mann, *J. Am. Chem. Soc.* **2004**, *126*, 15295 – 15308.
[2] R. J. Chesterfield, C. R. Newman, T. M. Pappenfus, P. C. Ewbank, M. H. Haukaas, K. R. Mann, L. L. Miller, C. D. Frisbie, *Adv. Mater.* **2003**, *15*, 1278 – 1282.
[3] a) R. Ponce Ortiz, J. Casado, V. Hernández, J. T. López Navarrete, E. Ortí, P. M. Viruela, B. Milián, S. Hotta, G. Zotti, S. Zecchin, B. Vercelli, *Adv. Funct. Mater.* **2006**, *16*, 531 – 536; b) G. Zotti, S. Zecchin, B. Vercelli, A. Berlin, J. Casado, V. Hernández, R. P. Ortiz, J. T. López Navarrete, E. Ortí, P. M. Viruela, B. Milián, *Chem. Mater.* **2006**, *18*, 1539 – 1545.
[4] T. Izumi, S. Kobashi, K. Takimiya, Y. Aso, T. Otsubo, *J. Am. Chem. Soc.* **2003**, *125*, 5286 – 5287.
[5] T. Takahashi, K. Matsuoka, K. Takimiya, T. Otsubo, Y. Aso, *J. Am. Chem. Soc.* **2005**, *127*, 8928 – 8929.
[6] a) T. Kubo, A. Shimizu, M. Sakamoto, M. Uruichi, K. Yakushi, M. Nakano, D. Shiomi, K. Sato, T. Takui, Y. Morita, K. Nakasuji, *Angew. Chem.* **2005**, *117*, 6722 – 6726; *Angew. Chem. Int. Ed.* **2005**, *44*, 6564 – 6568; b) T. Kubo, M. Sakamoto, K. Nakasuji, *Polyhedron* **2005**, *24*, 2522 – 2527; c) T. Kubo, A. Shimizu, M. Uruichi, K. Yakushi, M. Nakano, D. Shiomi, K. Sato, T. Takui, Y. Morita, K. Nakasuji, *Org. Lett.* **2007**, *9*, 81 – 84.
[7] Restricted→unrestricted wave-function instability and singlet biradical character have been predicted within the B3LYP approach for other types of long conjugated systems, such as oligoacenes starting from hexacene and oligothiophene dications starting from sexithiophene; see: a) M. Bendikov, H. M. Duong, K. Starkey, K. N. Houk, E. Carter, F. Wudl, *J. Am. Chem. Soc.* **2004**, *126*, 7416 – 7417; b) S. S. Zade, M. Bendikov, *J. Phys. Chem. B* **2006**, *110*, 15839 – 15846.
[8] The CASSCF(2,2) wave function for the singlet ground state of a molecule with an even number of electrons is of the form $\Psi = c_1\,{}^1\Phi_0 + c_2\,{}^1\Phi_{\mathrm{H,H}\rightarrow\mathrm{L,L}} = c_1\,|\,\phi_{\mathrm{HOMO}}\,\bar{\phi}_{\mathrm{HOMO}}\,| + c_2\,|\,\phi_{\mathrm{LUMO}}\,\bar{\phi}_{\mathrm{LUMO}}\,|$ where the two active orbitals ϕ_{HOMO} and ϕ_{LUMO} are assumed to have different symmetries. A perfect singlet biradical state is represented by a wave function with equal weights ($c_1 = c_2 = 1/\sqrt{2}$ if Φ is normalized) for the two electronic configurations (50%:50% mixing). See: a) L. Salem, C. Rowland, *Angew. Chem.* **1972**, *84*, 86 – 106; *Angew. Chem. Int. Ed. Engl.* **1972**, *11*, 92 – 111; b) J. A. E. H. van Haare, E. Havinga, J. L. van Dongen, R. A. J. Janssen, J. Cornil, J.-L. Brédas, *Chem. Eur. J.* **1998**, *4*, 1509 – 1522.
[9] Ground-state singlet disjoint biradicals have been extensively discussed by Borden and others; a) W. T. Borden, E. R. Davidson, *J. Am. Chem. Soc.* **1977**, *99*, 4587 – 4594; b) W. T. Borden, H. Iwamura, J. Berson, *Acc. Chem. Res.* **1994**, *27*, 109 – 116; c) M. Filatov, S. Shaik, *J. Phys. Chem. A* **1999**, *103*, 8885 – 8889.
[10] The fact that the triplet state lies above the singlet state is a consequence of the disjoint nature of the biradical ground state. Biradicals with disjoint SOMOs have singlet and triplets states with similar energies, since the two unpaired electrons can be confined to different sets of atoms (with parallel or antiparallel configurations) to minimize the Coulombic energy coming from electrons of opposite spin (Pauli-allowed). Dynamic spin polarization, in this case, selectively stabilizes the singlet over the triplet state, violating Hund's rule and giving rise to singlet biradicals.[9]
[11] V. Hernández, J. Casado, F. J. Ramírez, G. Zotti, S. Hotta, J. T. López Navarrete, *J. Chem. Phys.* **1996**, *104*, 9271 – 9282.
[12] J. Casado, V. Hernández, S. Hotta, J. T. López Navarrete, *Adv. Mater.* **1998**, *10*, 1458 – 1461.

